THE JOURNAL OF PHYSICAL CHEMISTRY A

Article

pubs.acs.org/JPCA

Reactions of Fe^+ and FeO^+ with C_2H_2, C_2H_4, and C_2H_6: Temperature-Dependent Kinetics

Shaun G. Ard,[†] Joshua J. Melko,[†] Joseph A. Fournier,[‡] Nicholas S. Shuman,[†] and Albert A. Viggiano*[,†]

[†]Air Force Research Laboratory, Space Vehicles Directorate, Kirtland Air Force Base, Albuquerque, New Mexico 87117-5776, United States

[‡]Sterling Chemistry Laboratory, Yale University, P.O. Box 208107, New Haven, Connecticut 06520, United States

Supporting Information

ABSTRACT: We present the first temperature-dependent rate constants and branching ratios for the reactions of Fe^+ and FeO^+ with C_2H_2, C_2H_4, and C_2H_6 from 170 to 700 K. Fe^+ is observed to react only by association with the three hydrocarbons, with temperature dependencies of T^{-2} to T^{-3}. FeO^+ reacts with C_2H_2 and C_2H_4 at the collision rate over the temperature range, and their respective product branchings show similar temperature dependences. In contrast, the reaction with ethane is collisional at 170 K but varies as $T^{-0.5}$, while the product branching remains essentially flat with temperature. These variations in reactivity are discussed in terms of the published reactive potential surfaces. The effectiveness of Fe^+ as an oxygen-transfer catalyst toward the three hydrocarbons is also discussed.

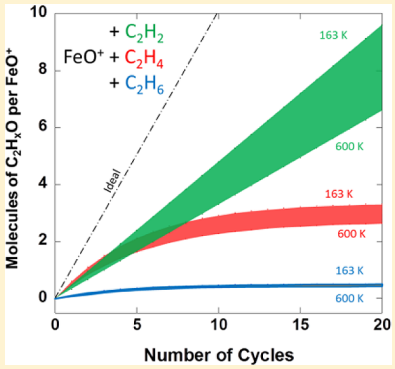

INTRODUCTION

The catalytic role of transition-metal ions in the activation of small molecules has garnered significant attention over the years.[1−17] In this light, gas-phase studies of ion−molecule reactions have led to many insights into the underlying mechanisms of numerous reactions involving transition metals, such as the concept of two-state reactivity.[2,4,18−23] While direct application of gas-phase studies to industrial processes is limited, the fundamental insight into the underlying reactions allows for a more rational and efficient development of catalysts applicable to the bulk phase. A prime example of this is the large-scale production of HCN from methane and ammonia, the understanding of which has greatly benefited from gas-phase studies of Pt^+ with both methane and ammonia.[24−26] Also important is the ability of gas-phase studies to lead to the development of efficient quantum chemical calculation methods by offering benchmarks for testing and refinement. Due to the significant computational scaling with respect to treatment of electron correlation for systems of this size, it is an important goal to find an acceptable compromise between accuracy and computational effort. The most commonly employed technique for transition-metal-containing systems, density functional theory (DFT), has performed with mixed results. Wide variations in calculated values are found to be highly dependent on thr functional and basis set employed, with little correlation to the system studied.[27−30]

We present here, for the first time, temperature-dependent kinetic data for the reactions of Fe^+ and FeO^+ with acetylene, ethylene, and ethane. Catalytic activation of C−C and C−H bonds is of considerable interest, and numerous studies have considered the mechanistic role of transition metals and their oxides in these reactions,[2,12,31−38] especially iron.[21,39−48] Here, we present the temperature dependence of the reaction rate constants and the product distributions in an effort to not only gain fundamental insight into the reaction mechanisms but additionally to allow for the assessment and refinement of the calculated potential energy surface for the reaction profiles.

EXPERIMENTAL METHODS

All measurements were performed on the Air Force Research Laboratory's variable temperature selected ion flow tube (VT-SIFT) instrument, which has been described in detail elsewhere.[49] Briefly, Fe^+ ions are created using an electron impact source in the presence of a 10% mixture of $Fe(CO)_5$ in He, with N_2O additionally supplied in the source for the formation of FeO^+. Ions are extracted and injected into a quadrupole mass filter where the desired ion, either Fe^+ or FeO^+, is mass selected. The ions are focused before introduction into a laminar flow tube via a Venturi inlet, where $\sim 10^4-10^5$ collisions with a He buffer gas act to thermalize the ions and carry them downstream. Previous work in our lab has shown that some excited electronic states of Fe^+ are inefficiently quenched[50] and may be present in the flow tube. FeO^+, however, is expected to be fully quenched due to its extra degrees of freedom. In either case, linear decays in parent ion signal on a semilogarithmic scale were observed over several orders of magnitude, indicative of a single rate constant (see the

Received: May 30, 2013
Revised: September 12, 2013
Published: September 12, 2013

   dx.doi.org/10.1021/jp405344w | J. Phys. Chem. A 2013, 117, 10178−10185

Supporting Information). The temperature of the flow tube is variable over a large range either by resistive heating devices (300−700 K), pulsed liquid nitrogen (120−220 K), or recirculating methanol chillers (220−300 K). Operating pressures of 0.4 Torr are maintained in the flow tube throughout all experiments, other than for verification of ternary reaction channels. The neutral reagent (C_2H_2, C_2H_4, or C_2H_6) is added 59 cm upstream of the end of the flow tube, with typical reaction times on the order of 4 ms, dependent on helium buffer flow (varied from 10 to 13 std. L min^{-1}) and temperature.

After traveling the length of the flow tube, the core of the flow is sampled through a truncated nose cone with a 2 mm aperture. The remainder of the flow is pumped away by a Roots pump through a throttled gate valve that acts to maintain the desired pressure within the flow tube. After the nose cone, the primary ions and product ions are guided by a lens stack to a quadrupole mass filter for analysis and are subsequently detected using an electron multiplier. Rate constants are derived by monitoring the decay of the primary ion as a function of the neutral reagent flow. Product branching is determined by monitoring the relative product formation as a function of neutral reagent and extrapolating to zero flow. Measurements were made from approximately 120 to 700 K, and temperature dependences of rate constants and product branching were determined. Errors in the rate constants are estimated to be ±25% absolute and ±15% relative to each other.[51] Errors in the product branching are estimated to be ±10%.

RESULTS AND DISCUSSION

1. $Fe^+ + C_2H_x$. The effective tertiary rate constants as a function of temperature for the reactions of Fe^+ with C_2H_2, C_2H_4, and C_2H_6 in 0.4 Torr of He are shown in Figure 1 and listed in Table 1. In all cases, the only primary product channel observed was association (e.g., the C_2H_2 reaction yielding $FeC_2H_2^+$). The association complexes were observed to further react by association, as has been previously reported.[44] The reaction of Fe^+ with ethane is known to have an exothermic channel producing $FeC_2H_4^+ + H_2$,[39] but this channel was not observed in this work or in previous SIFT work by Bohme et al.[44] This is unsurprising as the previously reported rate constant (~1/500 the collision rate constant) is at the lower end of our detection limit, and the pressures employed both in this work and that by Bohme et al. favor the association complex much more strongly than did the low-pressure beam experiments where that channel was observed.

Figure 2 shows the number density dependences of the rate constants at 300 K over the range accessible in the VT-SIFT. Least squares lines forced through zero are shown. The reactions of both acetylene and ethane show that that is correct within error, indicating that they are in the low-pressure limit,[52,53] and the termolecular rate constant is obtained from the slope. In contrast, the faster reaction with ethylene showed that forcing a zero intercept is a poor representation of the data, likely indicating that the reaction is intermediate between the low- (zero intercept) and high-pressure limits (flat with P). Because the observed C_2H_4 rate constants approach ~10% of the collision rate constant (compared to just 1−2% for the other reactions), perhaps this is not surprising. The alternative explanation for the nonzero intercept is that there is either a bimolecular or radiative association component to the reaction. Because no bimolecular products were observed, the former

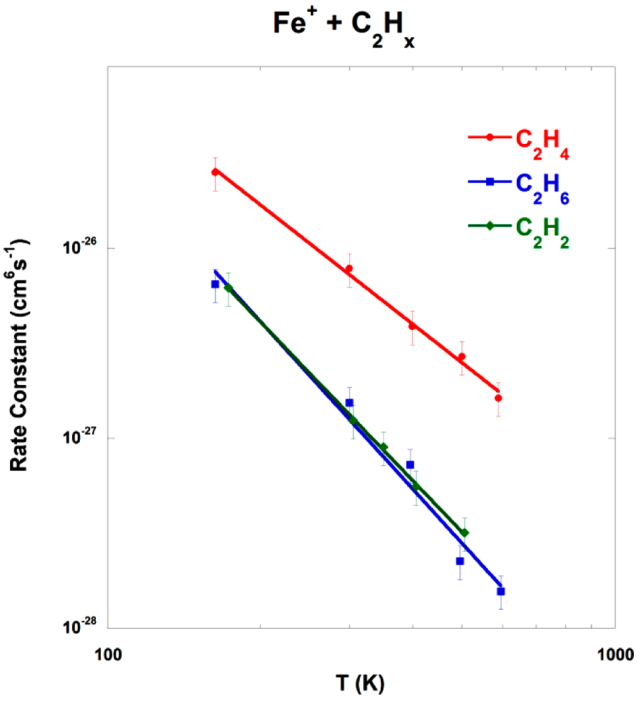

Figure 1. Tertiary rate constants for the reactions of Fe^+ with C_2H_2, C_2H_4, and C_2H_6 in 0.4 Torr of He. Pressure dependences show that the C_2H_2 and C_2H_6 values are true tertiary rate constants and that of C_2H_4 is an effective one in the falloff regime. Relative 15% error bars are shown.

Table 1. Effective Tertiary Rate Constants as a Function of Temperature, $k(T)$, for the Reactions of Fe^+ with C_2H_2, C_2H_4, and C_2H_6 in 0.4 Torr of He[a]

reaction	$k(T)$ cm^6 s^{-1}
$Fe^+ + C_2H_2 \rightarrow Fe(C_2H_2)^+$	$1.32 \times 10^{-27}(T/300)^{-2.8\pm0.2}$
$Fe^+ + C_2H_4 \rightarrow Fe(C_2H_4)^+$	$7.25 \times 10^{-27}(T/300)^{-2.1\pm0.2}$
$Fe^+ + C_2H_6 \rightarrow Fe(C_2H_6)^+$	$1.30 \times 10^{-27}(T/300)^{-2.9\pm0.2}$

[a]The C_2H_2 and C_2H_6 values are true termolecular values, while the C_2H_4 values are effective rate constants (see the text). Errors in the rate constants are estimated to be ±25% absolute and ±15% relative to each other.[51]

can be ruled out. The observed intercept would require an extremely large radiative rate, which is unlikely. Excited states of Fe^+ can also be ruled out as they would result in curvature in the decay, which is not observed over 1−3 orders of magnitude (see the Supporting Information) or different products. Thus, the reported rate constants for C_2H_2 and C_2H_6 are true termolecular values, and those for C_2H_4 are effective values. Unfortunately, we were unable to explore these reactions over a large enough pressure range to allow for precise modeling of the falloff curves.

Stationary points on the potential surfaces for all three reactions were calculated using DFT. While energy ordering of the various spin states is a well-known issue with density functional calculations on transition-metal systems, the calculations here employing B3LYP/TZVP[54,55] using the Gaussian 09 program suite[56] yield a $^6D-^4F$ energy splitting for Fe^+ of 0.29 eV, in reasonable agreement with the experimental spin−orbit average of 0.247 eV.[57,58] In agreement with previous calculations,[59−62] the ground state of each association complex was found to be quartet, as opposed to the

dx.doi.org/10.1021/jp405344w | J. Phys. Chem. A 2013, 117, 10178−10185

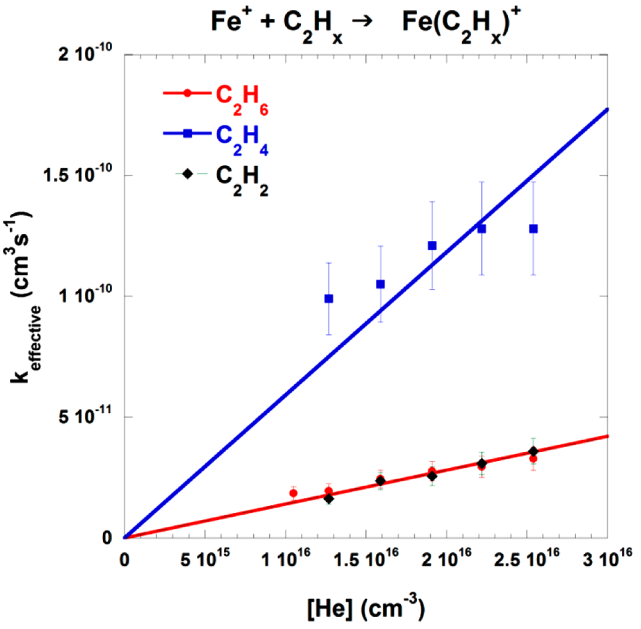

Figure 2. Effective bimolecular rate constant for the reactions of Fe^+ with C_2H_2, C_2H_4, and C_2H_6 as a function of He concentration. Least squares lines forced through zero are shown.

sextet ground state of the Fe^+ reactant. In Table 2, we list both the adiabatic bond dissociation energy (BDE) (i.e., the energy difference between the quartet association complex and the sextet Fe^+ reactants) and diabatic BDE (i.e., between the sextet association complex and the sextet Fe^+ reactants). For all three reactions, previously reported experimental BDEs fall about halfway in between the calculated adiabatic and diabatic BDEs.

Table 2. Calculated BDEs at the B3LYP/TZVP Level, as Well as the Published Experimentally Determined BDE for Each Association Product[a]

	calculated BDE (eV)		
association product	adiabatic	diabatic	experimental BDE (eV)
$Fe(C_2H_2)^+$	2.14	0.95	1.56[43,63]
$Fe(C_2H_4)^+$	2.12	1.00	1.5[64]
$Fe(C_2H_6)^+$	1.10	0.34	0.66[41]

[a]The adiabatic BDE assumes spin crossing from the sextet Fe^+ to quartet association complex, while the diabatic BDE assumes no spin crossing (i.e., sextet Fe^+ and sextet association complex).

The effective rate constants reported here for the association of Fe^+ with C_2H_2 and C_2H_6 are nearly identical over the entire temperature range, while the rate constant for C_2H_4 is approximately 5 times higher and declines less steeply with temperature; the latter is probably due to falloff effects. As previously discussed by Weishar[65] and Bohme,[44] the relative difference in rate constants can be rationalized in terms of the complex lifetime. $Fe(C_2H_2)^+$ and $Fe(C_2H_4)^+$ have similar bond dissociation energies,[43,63,64] but because $Fe(C_2H_4)^+$ has more degrees of freedom, it has a larger density of states at a given energy. As a result, calculating the unimolecular dissociation rate constants of the complexes via orbiting transition-state phase space theory indicates that $Fe(C_2H_4)^{+}$* has a longer lifetime than $Fe(C_2H_2)^{+}$* and thus a faster rate constant for the association. More accurate calculations need to know the rigidity factor,[66] and thus, these calculation allow only for a relative comparison. $Fe(C_2H_6)^+$ has the most complexity but also a much lower BDE (0.66 eV),[41] leading to a lifetime similar to that for $Fe(C_2H_2)^+$ (at the dissociation threshold). The phase space theory calculations are in agreement with the observed ordering of the rate constants. The relative difference in temperature dependencies is in part related to the reaction of Fe^+ with ethylene being in the falloff region; the high-pressure rate constant will have a lower temperature dependence than the low-pressure one.

Accurate modeling of the observed reactivity in this case is further complicated by the potential effects of intersystem crossing in these reactions. So-called two-state reactivity, where crossing to a different spin potential surface allows for a lower-energy path to products, has been observed in numerous reactions involving transition metals,[19,20] most notably with Fe^+,[30,67−69] though the extent of the role that it plays is hard to predict. In determining the BDE of $Fe(C_2H_4)^+$, Armentrout reports enough diabatic (spin-conserving) nature to the observed thresholds that the reported BDE is adjusted by the $^4Fe^+$−$^6Fe^+$ energy splitting.[64] Conversely, we have recently reported on the reaction of Fe^+ with N_2O, finding that a significant likelihood of curve crossing from the sextet to quartet surface is needed to model the observed reaction rate constants.[70] Quantitative understanding of the interplay of spin states in reactions of this type is still in its infancy; thus, attempts to model this system in greater detail would be premature.

Table 3. Rate Constants (k), Product Branching, Collision Rate Constant (k_{coll}), and Reaction Efficiency (k/k_{Coll}) for the Bimolecular Reactions of FeO^+ with Acetylene, Ethylene, and Ethane at 300 K[a]

		product branching					
reaction		this work	lit.	k (300 K) cm^3 s^{-1}	k_{coll} cm^3 s^{-1}	k/k_{coll} (300 K)	T dep
$FeO^+ + C_2H_4$	→ $Fe^+ + C_2H_2O$	0.43	0.5[b]	9.85×10^{-10}	1.06×10^{-9}	0.93	$\sim T^0$
	→ $FeCH_2^+ + CO$	0.57	0.5[b]				
$FeO^+ + C_2H_4$	→ $Fe^+ + C_2H_4O$	0.60	0.82[c]	1.08×10^{-9}	1.08×10^{-9}	1.00	$\sim T^0$
	→ $FeCH_2^+ + CH_2O$	0.26	0.11[c]				
	→ $FeC_2H_2^+ + H_2O$	0.04	0.04[c]				
	→ $FeCO^+ + CH_4$	0.10	0.03[c]				
$FeO^+ + C_2H_6$	→ $Fe^+ + C_2H_6O$	0.12	0.10,[d] 0.12[e]	8.56×10^{-10}, 8.4×10^{-10}[d]	1.07×10^{-9}	0.80	$T^{-0.47\pm0.15}$
	→ $FeC_2H_4^+ + H_2O$	0.67	0.70[d] 0.67[e]				
	→ $FeH_2^+ + C_2H_4$	0.21	0.20,[d] 0.12[e]				

[a]Errors in the rate constants are estimated to be ±25% absolute and ±15% relative to each other.[51] Errors in the product branching are estimated to be ±10%. The temperature dependence (T dep) is also given. [b]From ref 13. [c]From ref 72. [d]From ref 71. [e]From ref 45.

dx.doi.org/10.1021/jp405344w | J. Phys. Chem. A 2013, 117, 10178−10185

2. $FeO^+ + C_2H_x$. The rate constants and product branching observed for the bimolecular reactions of FeO^+ with acetylene, ethylene, and ethane at 300 K are listed in Table 3, as are previously published values, where available.[13,45,71,72] The reaction efficiencies, defined as the ratio of the experimentally measured rate constant to the collision rate constant as calculated by the parametrized Su and Chesnavich method,[73] are shown in Figure 3 from 170 to 700 K. Both acetylene and ethylene react at the collision rate over the entire temperature range. Ethane reacts at the collision rate at 170 K, and the efficiency decreases as approximately $T^{-1/2}$. Each reaction yields several products, which are discussed below.

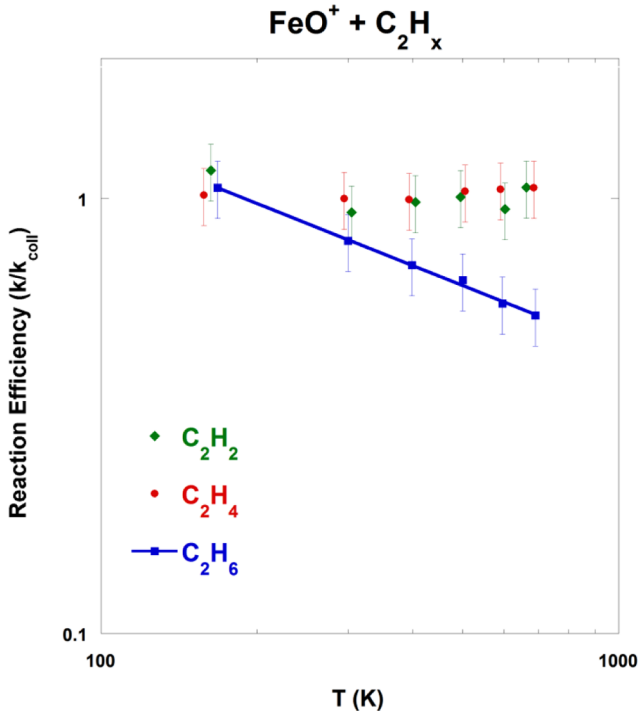

Figure 3. Reaction efficiencies, defined as the ratio of the experimentally measured rate constant to the calculated collision rate constant, for the reaction of FeO^+ with acetylene, ethylene, and ethane from 170 to 700 K.

The behavior of these reactions is entirely consistent with calculations of the surfaces that have been published elsewhere. Reaction pathways for FeO^+ with acetylene[47] and ethane[48] have been published by Zhao et al. employing density functional methods. Sun et al. further calculated the energetics of DFT-optimized stationary points on the reaction surface at the CCSD(T) level for the reaction with ethane; they also introduced a potentially competitive direct hydrogen abstraction pathway toward the oxygen-transfer product ethanol.[42] This pathway has a calculated barrier that is competitive with the concerted pathway, though just above the reactant energy. To the best of our knowledge, no surface for the reaction with ethylene has been reported.

For the acetylene reaction, the calculated highest-energy transition-state barrier for the lowest-energy pathway is 1.33 eV below the reactants, while the products lie 2.11 and 2.16 eV below.[47] This highly exothermic reaction is only minimally hindered kinetically and therefore would be expected to proceed with very high efficiency and minimal variation over this temperature range, in excellent agreement with what we observe. While no surface is available for the reaction with ethylene, a similar behavior of the rate constant strongly suggests that the largest transition-state barrier lies well below the initial reactants as well. For the reaction of FeO^+ with ethane, the behavior of the rate constant is in better agreement with the surface published by Zhao et al.[48] In this case, the largest transition-state barrier is 0.55 eV below the reactants, whereas Sun et al. found the largest transition-state barrier on the lowest-energy pathway to be only 0.069 eV below the reactants.[42] In both cases, traversing the lowest-energy transition-state barrier requires crossing from the sextet surface to the quartet surface, potentially an example of two-state reactivity.[19] Sun et al. also calculated the spin−orbit coupling at the crossing point just prior to the 0.069 eV exothermic barrier, suggesting that the crossing may be quite facile.[42] However, a near-thermoneutral barrier such as this is inconsistent with a reaction as efficient as that observed, even assuming that the crossing ensues with no kinetic hindrance. The present measurements are therefore more in line with the pure DFT calculations than the DFT optimizations with CCSD(T) single-point energies. The temperature dependence of this reaction is explained by rotational channel switching.[74] As the temperature rises, both the internal energy distribution and the J distribution of the system are shifted upward, the latter due to the increasing likelihood of large impact parameter collisions surmounting the centrifugal entrance barrier. Both factors favor returning to reactants through the loose entrance transition state, as opposed to continuing to products over the tighter transition state, the rotational barrier for which rises more steeply with J.

The product branching for the reactions of FeO^+ with acetylene, ethylene, and ethane from 170 to 700 K are shown in Figures 4−6, respectively. The reaction of FeO^+ with ethane shows strong selectivity (~67%) for production of $FeC_2H_4^+$

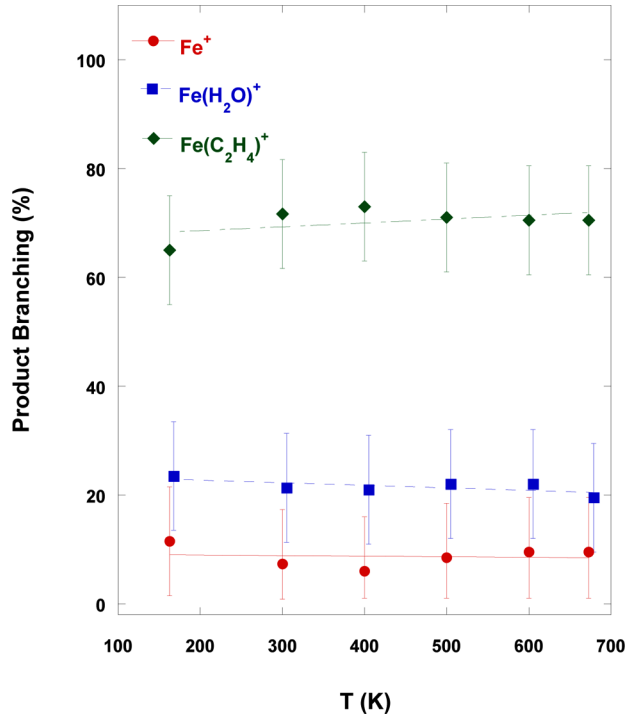

Figure 4. Product branching for the reaction of FeO^+ with ethane from 170 to 700 K. The fits shown are to guide the eye.

dx.doi.org/10.1021/jp405344w | J. Phys. Chem. A 2013, 117, 10178−10185

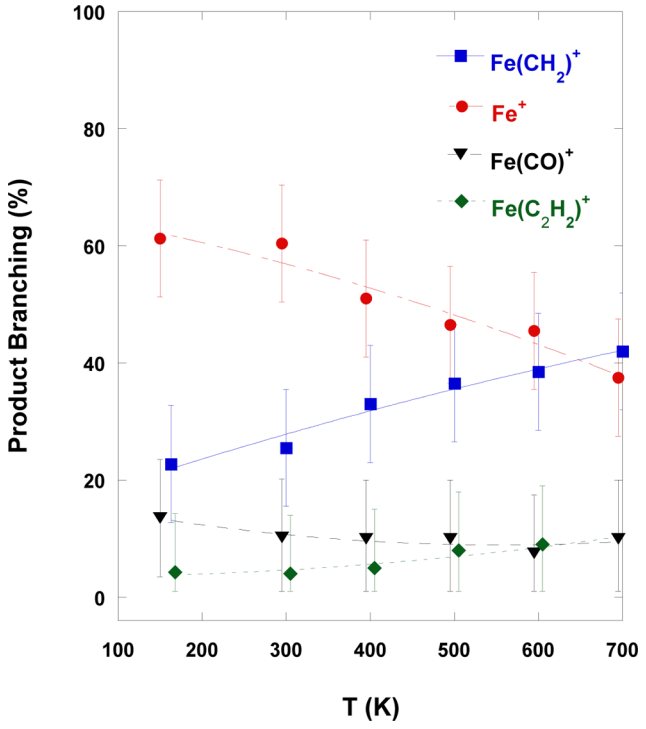

Figure 5. Product branching for the reaction of FeO^+ with ethylene from 170 to 700 K. The fits shown are to guide the eye.

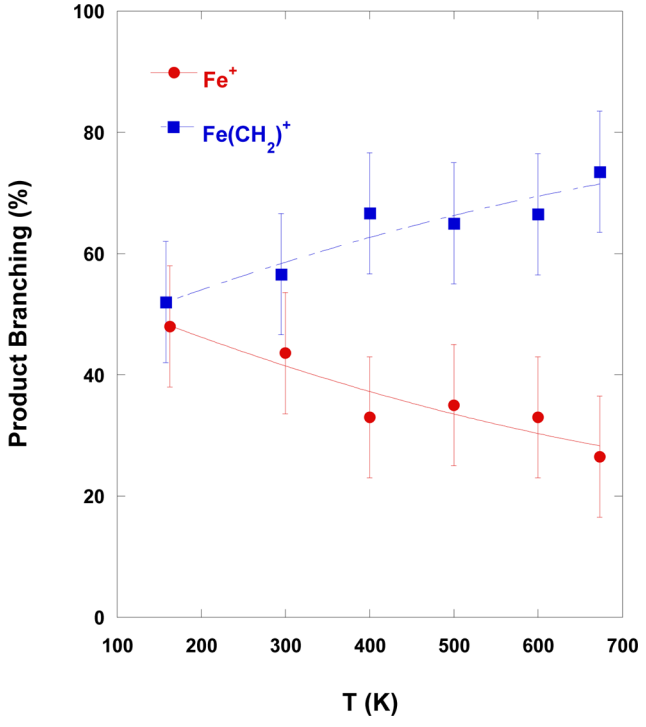

Figure 6. Product branching for the reaction of FeO^+ with acetylene from 170 to 700 K. The fits shown are to guide the eye.

and H_2O, with minor production of FeH_2O^+ and C_2H_4 (~21%) and very little production of Fe^+ and ethanol (~12%). The product branching remains essentially flat over the entire temperature range studied. This result agrees with the calculated thermodynamics for the reaction. The products are well-separated energetically, lying 2.25, 1.65, and 0.63 eV below ground-state reactants as calculated by Zhao for the $FeC_2H_4^+$, FeH_2O^+, and Fe^+ channels, respectively.[48] The small amount of energy added with temperature compared to these values is consistent with the small dependence of the branching on temperature. The direct hydrogen abstraction pathway to the Fe^+ + ethanol channel suggested by Sun et al.[42] is calculated to have a rate-limiting barrier just slightly higher than that for the concerted pathway (0.078 to −0.069 eV relative to the reactants, respectively), and the curve crossings prior to these barriers are expected to be comparable (spin−orbit coupling matrix elements of 315.5 and 306.6 cm^{-1}, respectively), indicative of this pathway likely being competitive. As discussed earlier, however, the high efficiency of this reaction is inconsistent with rate-limiting barriers near thermoneutral, such as these. Furthermore, the singular temperature dependence of the rate constant and especially the lack of temperature dependence in the product branching strongly support a single bottleneck to reactivity and thus a single mechanism over this temperature range. While the direct hydrogen abstraction pathway may be relevant at higher energies, near thermal energies, it appears to have no impact.

The product branchings for FeO^+ with ethylene and acetylene show striking similarities. The primary product ions formed in both cases are $FeCH_2^+$ and Fe^+, with the likely corresponding neutrals CH_2O and C_2H_4O for ethylene and CO and C_2H_2O for acetylene. Two additional minor products are also observed for the reaction with ethylene, $FeCO^+$ + CH_4 and $FeC_2H_2^+$ + H_2O. Both of these minor product channels remain small over our temperature range, with the former channel decreasing slightly and the latter increasing slightly. The oxygen-transfer channel resulting in Fe^+ formation is more prevalent in the reaction with ethylene than that with acetylene over all temperatures studied, though in both reactions, this channel decreased substantially with temperature while the $FeCH_2^+$ channel increased significantly.

Interpretation of the product branching ratios with respect to the published calculated surfaces is difficult. No surface has been published for the reaction with ethylene, and the calculated surface for the reaction with acetylene is extremely complicated, with numerous intermediates and transition states as well as several available Fe^+ channels due to varied conformations of the C_2H_2O neutral.[47] Producing Fe^+ and neutral CHCHO is calculated to be 1.19 eV endothermic and is unlikely to be involved under these experimental conditions. Changing the neutral isomer to CHCOH makes the reaction 0.57 eV exothermic, and production of CH_2CO is 2.16 eV exothermic. This is just 0.05 eV below the $FeCH_2^+$ + CO channel. Further complicating matters is the role of spin conservation in this reaction. As previously discussed, two-state reactivity is prevalent in many reactions involving transition-metal cations. The calculated surface for the reaction with acetylene involves numerous transition-state barriers that are considerably lower on the quartet surface as opposed to that on the sextet surface, indicative of potential two-state reactivity. Furthermore, the ground state of the $FeCH_2^+$ product is calculated to be quartet, while the ground state for the Fe^+ channels lie on the sextet surface, strongly suggesting that intersystem crossing between spin states has significant influence over the observed product branching.

Because a primary motive for this study is furthering our understanding of transition-metal cations in real world catalysts, it is informative to consider these reactions in this context. As an example, we consider the effectiveness of Fe^+ as an oxygen-transfer catalyst for these three hydrocarbons in combination

dx.doi.org/10.1021/jp405344w | J. Phys. Chem. A 2013, 117, 10178−10185

with the complementary reaction of $Fe^+ + N_2O$, which completes the catalytic cycle by producing FeO^+ in each reaction. We then calculate the number of oxidized products (alcohols) produced per cycle, accounting for products that may or may not lead to completion of the catalytic cycle through further reaction with N_2O. The results are shown in Figure 7. An ideal catalyst will produce one oxygen-transfer product per FeO^+ per cycle, and that is shown as the 1:1 line. The bands give the range for the two temperature extremes, highlighting the variation of product branching for the reactions over these temperatures. By far, the most efficient reaction is that with acetylene. While this does not equal the ideal case, because $FeCH_2^+$ is produced as a side product, the curve does not deviate from linear with increasing cycles because $FeCH_2^+$ will further react with N_2O to resupply Fe^+, and thus, the cycle is not poisoned. The poorest efficiency is seen in the reaction with ethane. After just a few cycles, the number of alcohol molecules produced saturates, indicating that no more are produced due to the poisoning by other channels. The low turnover number for this reaction, ~2.5,[45] is further compounded by the poor selectivity toward ethanol production. Oxygen transfer to ethylene is an interesting case. While the reaction is more selective toward oxygen transfer than the reaction with acetylene, the seemingly unimportant minor channels leading to $Fe(CO)^+$ and $Fe(C_2H_2)^+$ provide no way back to Fe^+ and are therefore dead channels. This limits the turnover number for this reaction to ~4.8, severely hindering the oxygen-transfer efficiency.

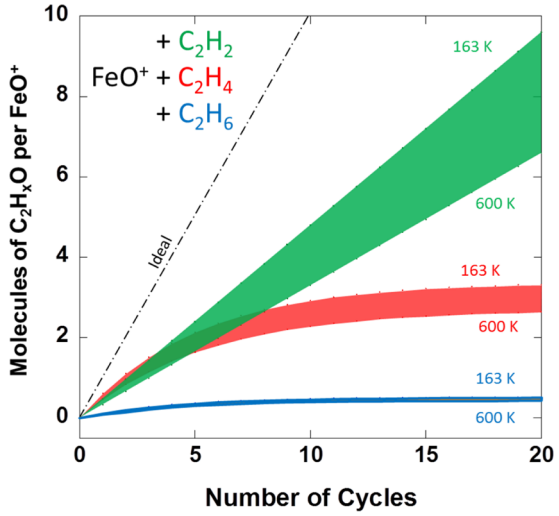

Figure 7. The relative efficiency of the oxygen-transfer process from 163 to 600 K for the reaction of FeO^+ with acetylene, ethylene, and ethane. An indication of an ideal catalyst producing one oxygen-transfer product per FeO^+ per cycle is shown as a dashed line. Product channels that lead to Fe^+, either initially or secondarily with further reaction with N_2O, are taken to resupply FeO^+ with unit efficiency.

CONCLUSIONS

We have studied the temperature dependence of the rate constants and product branching for the reactions of Fe^+ and FeO^+ with acetylene, ethylene, and ethane. Fe^+ is observed to react with the three hydrocarbons only by association. The relative differences in reaction rate constants are due to variations in the complex lifetime, while the variations in the T dependence are due to the reactions with acetylene and ethane being in the low-pressure limit for ternary reactions while the reaction with ethylene is in the falloff regime. The reactions of FeO^+ with the three hydrocarbons are very efficient; the reactions with acetylene and ethylene take place at the collisional limit over the entire temperature range studied, and the reaction with ethane is collisional at 170 K and falls off at $T^{-0.5}$. The product branching for the reactions of FeO^+ with acetylene and ethylene both showed a strong T dependence in the Fe^+ and the $FeCH_2^+$ producing channels, with the latter being favored at higher temperatures at the expense of the former, while the product branching of the ethane reaction remained static over our temperature range.

Each of the studied reactions was compared to published calculations of their reactive surfaces, where available. Detailed kinetic modeling was not performed due to the poorly quantified influence of two-state reactivity for the association reactions and extremely complicated nature of the surfaces for the reactive ones. Qualitative assessment was, however, possible. The high efficiency of the reactions with FeO^+ was in good agreement with the deeply submerged rate-limiting barriers calculated by Zhang et al. for the reactions with acetylene and ethane, with the latter being less submerged, in agreement with the slightly reduced reactivity. The product branching for the reaction with acetylene showed significant temperature dependence and is complicated by intersystem crossing between the quartet and sextet potential energy surfaces. The product branching for the ethane reaction is flat over our temperature range, consistent with the well-spaced, highly exothermic product channels calculated by Zhang et al. The static product branching, combined with the high efficiency of the reaction as well as a single temperature dependence, suggests that the alternate reaction pathway calculated by Sun et al. has little impact at thermal energies.

The comparison of the oxygen-transfer product channel for the reactions of FeO^+ with the three hydrocarbons highlights the importance of understanding the variation in product branching for these types of reactions. The reactions with both acetylene and ethylene exhibit a strong temperature dependence to their respective product branching and hence the selectivity of the reaction. More importantly, however, are channels that do not allow for a recycling of the catalytic ion. While the reaction of FeO^+ with ethylene shows more selectivity toward oxygen transfer than acetylene at all temperatures studied, the reaction with acetylene is significantly more productive as none of the products poison the catalytic cycle.

ASSOCIATED CONTENT

Supporting Information

Examples of raw data for the reactions of $Fe^+ + C_2H_4$ and $FeO^+ + C_2H_2$. This material is available free of charge via the Internet at http://pubs.acs.org.

AUTHOR INFORMATION

Corresponding Author

*E-mail: afrl.rvborgmailbox@kirtland.af.mil.

Notes

The authors declare no competing financial interest.

ACKNOWLEDGMENTS

This work was supported by the Air Force Office of Scientific Research under Project AFOSR-2303EP. J.J.M. and S.G.A.

acknowledge the support of the National Research Council. J.A.F. acknowledges the support of the Air Force Research Laboratory through the Space Scholars Program, as well as the Department of Defense for support through a National Defense Science and Engineering Graduate Fellowship.

REFERENCES

(1) Schwarz, H. Chemistry with Methane: Concepts Rather than Recipes. *Angew. Chem., Int. Ed.* **2011**, *50*, 10096−10115.
(2) Roithova, J.; Schroeder, D. Selective Activation of Alkanes by Gas-Phase Metal Ions. *Chem. Rev.* **2010**, *110*, 1170−1211.
(3) Roithova, J.; Schroder, D. Theory Meets Experiment: Gas-Phase Chemistry of Coinage Metals. *Coord. Chem. Rev.* **2009**, *253*, 666−677.
(4) Lang, S. M.; Bernhardt, T. M. Gas Phase Metal Cluster Model Systems for Heterogeneous Catalysis. *Phys. Chem. Chem. Phys.* **2012**, *14*, 9255−9269.
(5) Bernhardt, T. M. Gas-Phase Kinetics and Catalytic Reactions of Small Silver and Gold Clusters. *Int. J. Mass Spectrom.* **2005**, *243*, 1−29.
(6) Wasserscheid, P.; Keim, W. Ionic Liquids — New "Solutions" for Transition Metal Catalysis. *Angew. Chem., Int. Ed.* **2000**, *39*, 3772−3789.
(7) Zaera, F. Surface Chemistry of Hydrocarbon Fragments on Transition Metals: Towards Understanding Catalytic Processes. *Catal. Lett.* **2003**, *91*, 1−10.
(8) Miller, D. M.; Buettner, G. R.; Aust, S. D. Transition-Metals as Catalysts of Autooxidation Reactions. *Free Radical Biol. Med.* **1990**, *8*, 95−108.
(9) Roucoux, A.; Schulz, J.; Patin, H. Reduced Transition Metal Colloids: A Novel Family of Reusable Catalysts? *Chem. Rev.* **2002**, *102*, 3757−3778.
(10) Hill, C. L.; Prossermccartha, C. M. Homogeneous Catalysis by Transition-Metal Oxygen Anion Clusters. *Coord. Chem. Rev.* **1995**, *143*, 407−455.
(11) Niu, S. Q.; Hall, M. B. Theoretical Studies on Reactions of Transition-Metal Complexes. *Chem. Rev.* **2000**, *100*, 353−405.
(12) Conley, B. L.; Tenn, W. J.; Young, K. J. H.; Ganesh, S. K.; Meier, S. K.; Ziatdinov, V. R.; Mironov, O.; Oxgaard, J.; Gonzales, J.; Goddard, W. A.; et al. Design and Study of Homogeneous Catalysts for the Selective, Low Temperature Oxidation of Hydrocarbons. *J. Mol. Catal. A: Chem.* **2006**, *251*, 8−23.
(13) Kappes, M. M.; Staley, R. H. Gas-Phase Oxidation Catalysis by Transition-Metal Cations. *J. Am. Chem. Soc.* **1981**, *103*, 1286−1287.
(14) Bond, G. C.; Thompson, D. T. Catalysis by Gold. *Catal. Rev.: Sci. Eng.* **1999**, *41*, 319−388.
(15) Bohme, D. K.; Schwarz, H. Gas-Phase Catalysis by Atomic and Cluster Metal Ions: The Ultimate Single-Site Catalysts. *Angew. Chem., Int. Ed.* **2005**, *44*, 2336−2354.
(16) Widegren, J. A.; Finke, R. G. A Review of the Problem of Distinguishing True Homogeneous Catalysis from Soluble or Other Metal-Particle Heterogeneous Catalysis under Reducing Conditions. *J. Mol. Catal. A: Chem.* **2003**, *198*, 317−341.
(17) Schwarz, K. E. H. Organometallic Chemistry in the Gas-Phase. *Chem. Rev.* **1991**, *91*, 1121−1177.
(18) Somorjai, G. A.; Park, J. Y. Molecular Factors of Catalytic Selectivity. *Angew. Chem., Int. Ed.* **2008**, *47*, 9212−9228.
(19) Schroder, D.; Shaik, S.; Schwarz, H. Two-State Reactivity as a New Concept in Organometallic Chemistry. *Acc. Chem. Res.* **2000**, *33*, 139−145.
(20) Shaik, S.; Danovich, D.; Fiedler, A.; Schroder, D.; Schwarz, H. 2-State Reactivity in Organometallic Gas-Phase Ion Chemistry. *Helv. Chim. Acta* **1995**, *78*, 1393−1407.
(21) Armentrout, P. B.; Tjelta, B. L. Dramatic Ligand Effects on Gas-Phase Transition-Metal Reactivity and Selectivity: Studies of Fe^+, $Fe^+(H_2O)$, and $Fe^+(CO)$ with Propane. *Organometallics* **1997**, *16*, 5372−5374.
(22) Villano, S. M.; Eyet, N.; Lineberger, W. C.; Bierbaum, V. M. Gas-Phase Carbene Radical Anions: New Mechanistic Insights. *J. Am. Chem. Soc.* **2008**, *130*, 7214−7215.
(23) Fiedler, A.; Schroder, D.; Shaik, S.; Schwarz, H. Electronic-Structures and Gas-Phase Reactivities of Cationic Late-Transition-Metal Oxides. *J. Am. Chem. Soc.* **1994**, *116*, 10734−10741.
(24) Hasenberg, D.; Schmidt, L. D. HCN Synthesis from CH_4 and NH_3 on Platinum. *J. Catal.* **1986**, *97*, 156−168.
(25) Horn, R.; Mestl, G.; Thiede, M.; Jentoft, F. C.; Schmidt, P. M.; Bewersdorf, M.; Weber, R.; Schlogl, R. Gas Phase Contributions to the Catalytic Formation of HCN from CH_4 and NH_3 over Pt: An In Situ Study by Molecular Beam Mass Spectrometry with Threshold Ionization. *Phys. Chem. Chem. Phys.* **2004**, *6*, 4514−4521.
(26) Koberste, E. Model Reactor Studies of Hydrogen-Cyanide Synthesis from Methane and Ammonia. *Ind. Eng. Chem. Process Des. Dev.* **1973**, *12*, 444−448.
(27) Cohen, A. J.; Mori-Sánchez, P.; Yang, W. Challenges for Density Functional Theory. *Chem. Rev.* **2011**, *112*, 289−320.
(28) Guell, M.; Luis, J. M.; Sola, M.; Swart, M. Importance of the Basis Set for the Spin-State Energetics of Iron Complexes. *J. Phys. Chem. A* **2008**, *112*, 6384−6391.
(29) Wagner, L. K. Transition Metal Oxides using Quantum Monte Carlo. *J. Phys.: Condens. Matter* **2007**, *19*, 343201−343214.
(30) Chiodo, S.; Kondakova, O.; Michelini, M. D.; Russo, N.; Sicilia, E.; Irigoras, A.; Ugalde, J. M. Theoretical Study of Two-State Reactivity of Transition Metal Cations: The "Difficult" Case of Iron Ion Interacting with Water, Ammonia, and Methane. *J. Phys. Chem. A* **2004**, *108*, 1069−1081.
(31) Vankoppen, P. A. M.; Brodbeltlustig, J.; Bowers, M. T.; Dearden, D. V.; Beauchamp, J. L.; Fisher, E. R.; Armentrout, P. B. C−H Bond Activation as the Initial Step in the CO^+-Mediated Demethanation of Propane: The Critical Role of Angular-Momentum at the Rate-Limiting Transition-State. *J. Am. Chem. Soc.* **1990**, *112*, 5663−5665.
(32) Vankoppen, P. A. M.; Brodbeltlustig, J.; Bowers, M. T.; Dearden, D. V.; Beauchamp, J. L.; Fisher, E. R.; Armentrout, P. B. Transition-Metal Ion Mediated C−H and C−C Bond Activation of Alkanes: Dynamic Coupling between Entrance and Exit Channel Transition-States. *J. Am. Chem. Soc.* **1991**, *113*, 2359−2369.
(33) Tjelta, B. L.; Armentrout, P. B. Ligand Effects in σ-Bond Activation by Transition Metal-Ligand Complexes. *J. Am. Chem. Soc.* **1995**, *117*, 5531−5533.
(34) Schroder, D.; Schwarz, H. C−H and C−C Bond Activation by Bare Transition-Metal Oxide Cations in the Gas-Phase. *Angew. Chem., Int. Ed. Engl.* **1995**, *34*, 1973−1995.
(35) Akhmedov, V. M.; Al-Khowaiter, S. H. Recent Advances and Future Aspects in the Low-Temperature Conversion of Saturated Hydrocarbons. *Catal. Rev.: Sci. Eng.* **2002**, *44*, 455−498.
(36) Godula, K.; Sames, D. C−H Bond Functionalization in Complex Organic Synthesis. *Science* **2006**, *312*, 67−72.
(37) Parke, L. G.; Hinton, C. S.; Armentrout, P. B. Energetics and Mechanisms of C−H Bond Activation by a Doubly Charged Metal Ion: Guided Ion Beam and Theoretical Studies of $Ta^{2+} + CH_4$. *J. Phys. Chem. A* **2008**, *112*, 10469−10480.
(38) Schroder, D.; Schwarz, H. FeO^+ Activates Methane. *Angew. Chem., Int. Ed.* **1990**, *12*, 1433−1434.
(39) Schultz, R. H.; Elkind, J. L.; Armentrout, P. B. Electronic Effects in C−H and C−C Bond Activation: State-Specific Reactions of $Fe^+(^6D,^4F)$ with Methane, Ethane, and Propane. *J. Am. Chem. Soc.* **1988**, *110*, 411−423.
(40) Schultz, R. H.; Armentrout, P. B. The Gas-Phase Thermochemistry of FeH. *J. Chem. Phys.* **1991**, *94*, 2262−2268.
(41) Schultz, R. H.; Armentrout, P. B. Threshold Collisional Activation of $FeC_2H_6^+$: Fe^+·Ethane vs Fe^+·Dimethyl Structures. *J. Phys. Chem.* **1992**, *96*, 1662−1667.
(42) Sun, X. L.; Huang, X. R.; Li, J. L.; Huo, R. P.; Sun, C. C. Mechanism Insights of Ethane C−H Bond Activations by Bare $[Fe^{III}{=}O]^+$: Explicit Electronic Structure Analysis. *J. Phys. Chem. A* **2012**, *116*, 1475−1485.
(43) Schroder, D.; Schwarz, H. Ligand Effects as Probes for Mechanistic Aspects of Remote C−H Bond Activation by Iron(I) Cations in the Gas-Phase. *J. Organomet. Chem.* **1995**, *504*, 123−135.

(44) Baranov, V.; Becker, H.; Bohme, D. K. Intrinsic Coordination Properties of Iron: Gas-Phase Ligation of Ground-State Fe^+ with Alkanes, Alkenes, and Alkynes and Intramolecular Interligand Interactions Mediated by Fe^+. *J. Phys. Chem. A* **1997**, *101*, 5137−5147.
(45) Schroder, D.; Schwarz, H. Fe^+-Catalyzed Gas-Phase Oxidation of Ethane by N_2O. *Angew. Chem., Int. Ed.* **1990**, *29*, 1431−1433.
(46) Schroder, D.; Eller, K.; Prusse, T.; Schwarz, H. Ligand-Enhanced Selectivity in the CH/CC Bond Activation of Ketones by Iron(I) Ions in the Gas Phase. *Organometallics* **1991**, *10*, 2052−2055.
(47) Zhao, L. M.; Wang, Y.; Guo, W. Y.; Shan, H. H.; Lu, X. Q.; Yang, T. Theoretical Investigation of the Fe^+-Catalyzed Oxidation of Acetylene by N_2O. *J. Phys. Chem. A* **2008**, *112*, 5676−5683.
(48) Zhao, L. M.; Guo, W. Y.; Liu, Z. C.; Li, Y. Y.; Lu, X. Q. Theoretical Study of the Gas-Phase Fe^+-Mediated Oxidation of Ethane by N_2O. *Theor. Chem. Acc.* **2011**, *128*, 349−358.
(49) Viggiano, A. A.; Morris, R. A.; Dale, F.; Paulson, J. F.; Giles, K.; Smith, D.; Su, T. Kinetic-Energy, Temperature, and Derived Rotational Temperature Dependences for the Reactions of $KR^+(^2P_{3/2})$ and AR^+ with HCL. *J. Chem. Phys.* **1990**, *93*, 1149−1157.
(50) Melko, J. J.; Ard, S. G.; Fournier, J. A.; Shuman, N. S.; Troe, J.; Viggiano, A. A. Exploring the Reactions of Fe^+ and FeO^+ with NO and NO_2. *J. Phys. Chem. A* **2012**, *116*, 11500−11508.
(51) Dotan, I.; Viggiano, A. A.; Morris, R. A. Rotational Temperature Dependence of the Branching Ratio for the Reaction of $Kr^+(^2P_{3/2})$ ions with HD. *J. Chem. Phys.* **1992**, *96*, 7445.
(52) Troe, J. Theory of Thermal Unimolecular Reactions in the Fall-Off Range. 1. Strong Collision Rate Constants. *Ber. Bunsen-Ges. Phys. Chem. Chem. Phys.* **1983**, *87*, 161−169.
(53) Gilbert, R. G.; Luther, K.; Troe, J. Theory of Thermal Unimolecular Reactions in the Fall-Off Range. 2. Weak Collision Rate Constants. *Ber. Bunsen-Ges. Phys. Chem. Chem. Phys.* **1983**, *87*, 169−177.
(54) Becke, A. D. DFT Basis Set Theory. *Phys. Rev. A* **1988**, *38*, 3098−3100.
(55) Lee, C.; Yang, W.; Parr, R. G. Development of the Colle−Salvetti Correlation-Energy Formula into a Functional of the Electron Density. *Phys. Rev. B* **1988**, *37*, 785−789.
(56) Frisch, M. J.; Trucks, G. W.; Schlegel, H. B.; Scuseria, G. E.; Robb, M. A.; Cheeseman, J. R.; Scalmani, G.; Barone, V.; Mennucci, B.; Petersson, G. A.; et al. *Gaussian 09*; Gaussian, Inc.: Wallingford, CT, 2009.
(57) Corliss, C.; Sugar, J. Energy Levels of Iron, Fe I through Fe XXVI. *J. Phys. Chem. Ref. Data* **1982**, *11*, 135−241.
(58) Sugar, J. *Atomic Energy Levels of the Iron-Period Elements, Potassium Through Nickel*; American Chemical Society and the American Institute of Physics for the National Bureau of Standards: New York, 1985; Vol. *14*.
(59) Klippenstein, S. J.; Yang, C. N. Density Functional Theory Predictions for the Binding of Transition Metal Cations to Pi Systems: from Acetylene to Coronene and Tribenzocyclyne. *Int. J. Mass Spectrom.* **2000**, *201*, 253−267.
(60) Holthausen, M. C.; Fiedler, A.; Schwarz, H.; Koch, W. Mechanism of the Fe^+ Mediated C−C and C−H Bond Activations in Ethane from a Theoretical Viewpoint. *Angew. Chem., Int. Ed. Engl.* **1995**, *34*, 2282−2285.
(61) Barsch, S.; Schroder, D.; Schwarz, H. How Does Fe^+ Activate Ethylsilane? A Theoretical Study in Comparison with Experiments. *Int. J. Mass Spectrom.* **2000**, *202*, 363−379.
(62) Hendrickx, M.; Gong, K.; Vanquickenborne, L. Theoretical Study of the Molecular Complexes of Fe^+ with Small Alkanes. *J. Chem. Phys.* **1997**, *107*, 6299−6305.
(63) Surya, P. I.; Ranatunga, D. R. A.; Freiser, B. S. Infrared Multiphoton Dissociation of $MC_4H_6^+$ [M = Fe, Co, or Ni; C_4H_6 = 1,3-Butadiene or $(C_2H_2)(C_2H_4)$]. *J. Am. Chem. Soc.* **1997**, *119*, 3351−3357.
(64) Sievers, M. R.; Jarvis, L. M.; Armentrout, P. B. Transition-Metal Ethene Bonds: Thermochemistry of $M^+(C_2H_4)_n$(M = Ti−Cu, n = 1 and 2) Complexes. *J. Am. Chem. Soc.* **1998**, *120*, 1891−1899.
(65) Tonkyn, R.; Ronan, M.; Weisshaar, J. C. Multicollision Chemistry of Gas-Phase Transition-Metal Ions with Small Alkanes: Rate Constants and Product Branching at 0.75 Torr of HE. *J. Phys. Chem.* **1988**, *92*, 92−102.
(66) Troe, J. Towards Simplified Thermal and Specific Rigidity Factors for Ion−Molecule Reactions and Ion Fragmentations. *Z. Phys. Chem.* **2009**, *223*, 347−357.
(67) Schultz, R. H.; Armentrout, P. B. Nonadiabatic Behavior of a Transition-Metal System: Exothermic Reactions of $Fe^+(^6D,^4F)$ and Propane. *J. Phys. Chem.* **1987**, *91*, 4433−4435.
(68) Schroder, D.; Schwarz, H.; Clemmer, D. E.; Chen, Y. M.; Armentrout, P. B.; Baranov, V. I.; Bohme, D. K. Activation of Hydrogen and Methane by Thermalized FeO^+ in the Gas Phase as Studied by Multiple Mass Spectrometric Techniques. *Int. J. Mass Spectrom. Ion Process.* **1997**, *161*, 175−191.
(69) Clemmer, D. E.; Chen, Y. M.; Khan, F. A.; Armentrout, P. B. State-Specific Reactions of $Fe^+(a^6D,a^4F)$ with D_2O and Reactions of FeO^+ with D_2. *J. Phys. Chem.* **1994**, *98*, 6522−6529.
(70) Melko, J. J.; Ard, S. G.; Fournier, J. A.; Li, J.; Shuman, N. S.; Guo, H.; Troe, J.; Viggiano, A. A. Iron Cation Catalyzed Reduction of N_2O by CO: Gas-Phase Temperature Dependent Kinetics. *Phys. Chem. Chem. Phys.* **2013**, *15*, 11257−11267.
(71) Jackson, T. C.; Jacobson, D. B.; Freiser, B. S. Gas-Phase Reactions of FeO^+ with Hydrocarbons. *J. Am. Chem. Soc.* **1984**, *106*, 1252−1257.
(72) Buckner, S. W.; Gord, J. R.; Freiser, B. S. Gas-Phase Chemistry of Transition Metal-Imido and Metal−Nitrene Ion Complexes: Oxidative Addition of N−H Bonds in NH_3 and Transfer of NH from a Metal Center to an Alkene. *J. Am. Chem. Soc.* **1988**, *110*, 6606−6612.
(73) Su, T.; Chesnavich, W. J. Parametrization of the Ion−Polar Molecule Collision Rate Constant by Trajectory Calculations. *J. Chem. Phys.* **1982**, *76*, 5183−5185.
(74) Troe, J. Statistical Adiabatic Channel Model of Ion Neutral Dipole Capture Rate Constants. *Chem. Phys. Lett.* **1985**, *122*, 425−430.